Materials Science & Engineering A 680 (2017) 1–12

Contents lists available at ScienceDirect

Materials Science & Engineering A

journal homepage: www.elsevier.com/locate/msea

Mechanism research on accelerated embrittlement phenomenon of a warm-deformed Cr-Mn-Ni-Mo-N austenitic stainless steel

H.P. Qu[a,*], H.T. Chen[a], C.X. Cao[b], Y.P. Lang[a], S.X. Zhang[a,c], Y. Cui[c]

[a] Institute of Special Steels, Central Iron and Steel Research Institute (CISRI), 76 Haidiannan Rd., Beijing, PR China
[b] Zhuozhou works, CISRI, 2 Huojunan Rd., Zhuozhou, Hebei, PR China
[c] School of Energy and Metallurgy, North China University of Science and Technology (NCUST), 46 Xinhuaxi Rd., Tangshan, Hebei, PR China

ARTICLE INFO

Keywords:
A. Embrittlement
B. Stainless steel
C. Bulk deformation
D. Dislocations
Orientation relationships
Precipitation

ABSTRACT

Effect of Ni, Mo content and warm deformation at 800 °C and 940 °C on $Cr_{23}C_6$ and Cr_2N precipitation behavior and room temperature (RT) impact toughness of a Mo-contained high N austenitic stainless steel was researched in this study. Results showed that mass percentage of Mo and Ni should be adjusted for sufficient γ phase region. The real precipitation kinetic of $Cr_{23}C_6$, Cr_2N and σ phase was affected by related elemental composition and deformation parameters. After the same aging, the embrittlement of warm-deformed specimen was accelerated due to obvious increase of intergranular $Cr_{23}C_6$ and discontinuous intragranular cellular Cr_2N precipitates. The accelerated embrittlement and $Cr_{23}C_6$ and Cr_2N precipitation were induced by high density dislocations generated during warm deformation. Dislocations dramatically increased adjacent precipitation nucleation opportunity and the growth rate of $Cr_{23}C_6$ and Cr_2N during aging process within corresponding sensitive temperature interval. Dislocation density also strongly affected growth direction and thickness of Cr_2N lamellae. Real forging parameters should be controlled to avoid this accelerated $Cr_{23}C_6$ and Cr_2N precipitation.

1. Introduction

Cr-Mn-N austenitic stainless steel (ASS) has long been researched as the candidate material for non-magnetic drilling collar (NMDC) due to its high strength, corrosion resistance and low raw material cost [1,2]. Mo was also added in the Cr-Mn-N system to promote the localized corrosion resistance in severe offshore drilling environment. Meanwhile, Ni also should be properly added to equilibrate the strong ferrite formation effect from Mo and ensure austenitic phase stability to meet the extremely low magnetic permeability standard of NMDC product [3,4]. During the industrial producing of NMDC, warm-forged rod slab was water-quenched without solid solution treatment to maximize deformation-induced strengthen effect [5]. Effect of warm deformation on precipitation behavior should therefore be carefully researched to avoid the potential mechanical properties deterioration, especially embrittlement tendency which could lead to fracture failure.

$M_{23}C_6$ and M_2N precipitation in high N ASSs has been researched for many years by means of thermal-dynamic calculation, aging experiment and microstructure observation [6–14]. For instance, Lee et al. observed the formation of continuous intergranular Cr_2N precipitate in a high N 18Cr-18Mn-2Mo-0.9N-0.04C steel after aging at 900 °C for longer than 10^3 s. As the aging time elongated to 10^5 s, Cr_2N grown towards inside the equiaxed grain and ultimately formed cellular morphology [15]. No $Cr_{23}C_6$ precipitate appeared as predicted in the calculated equilibrium phase diagram. σ phase precipitate appeared around the primary Cr_2N, of which the reason was attributed to the adjacent N depletion. Simmons proved that Cr_2N precipitates only appeared at grain boundary in a 19Cr-5Mn-3Mo-5Ni-0.7N-0.02C steel after aging at 700 °C for 3 h, while both the intergranular and intragranular cellular Cr_2N precipitates with the volume fraction of 40% was created after aging at 900 °C for the same time [16]. Zheng et al. discovered three types of $M_{23}C_6$ precipitates in a 0.3C-20Cr-11Mn-1Mo-0.35N steel after aging at 900 °C for up to 6×10^3 min, including equiaxed grain boundaries, twin boundaries and dislocations [17]. The relationship of $M_{23}C_6$ precipitates nucleation, growth and dispersion with aging time was also discussed. Based on these research, the thermal-dynamic characteristics of $Cr_{23}C_6$ and Cr_2N precipitation was strongly affected by the chemical composition, especially N and C content. With the elongated aging time, morphology evolution of $M_{23}C_6$ and Cr_2N precipitate was totally different.

Specimen preparation for precipitation research of above-mentioned literatures was usually by different aging after high temperature solid solution. Determined by the unique rapid forging manner of NMDC product, effect of warm deformation on $Cr_{23}C_6$ and Cr_2N

* Corresponding author.
E-mail address: quhuapeng0926@163.com (H.P. Qu).

http://dx.doi.org/10.1016/j.msea.2016.10.074
Received 22 August 2016; Received in revised form 18 October 2016; Accepted 19 October 2016
Available online 22 October 2016
0921-5093/

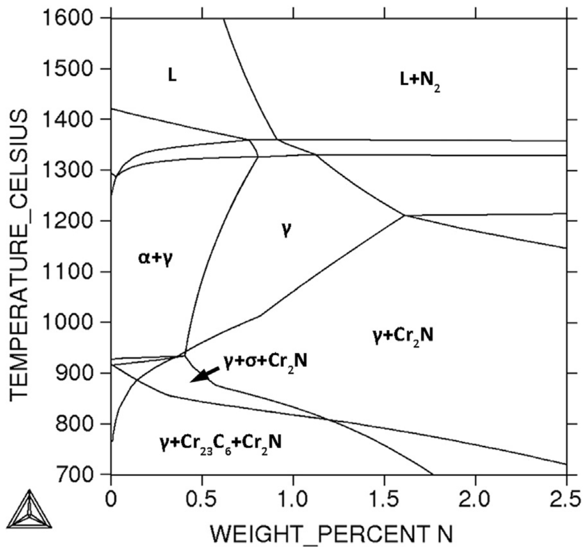

Fig. 1. Equilibrium phase diagram of the current steel with N content of 0.67 mass.%

Table 1
Chemical composition of the investigated high N ASS in mass percentage.

Elements	C	Cr	Mn	Ni	Mo	N	Si	P	S
Mass.%	0.053	19.87	21.33	2.21	0.55	0.67	0.22	0.0085	0.006

precipitation should be paid special attention. Unfortunately, insufficient research on this field was specially reported. Hong et al. found obvious $M_{23}C_6$ precipitation at grain boundary in a 0.11C-21Cr-16Mn-2Ni-0.65N stainless steel after hot compression at 850 °C with 60% engineering strain [18]. While no $M_{23}C_6$ precipitation was observed

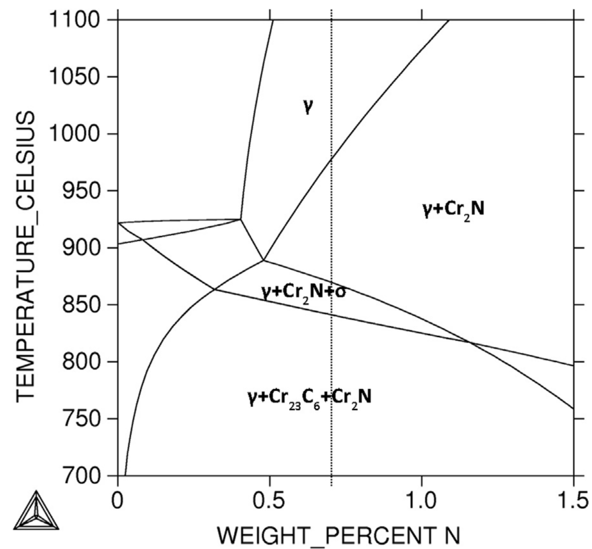

Fig. 3. Detailed calculation showed the important phase transformation of the current steel with N content of 0.67 mass.%.

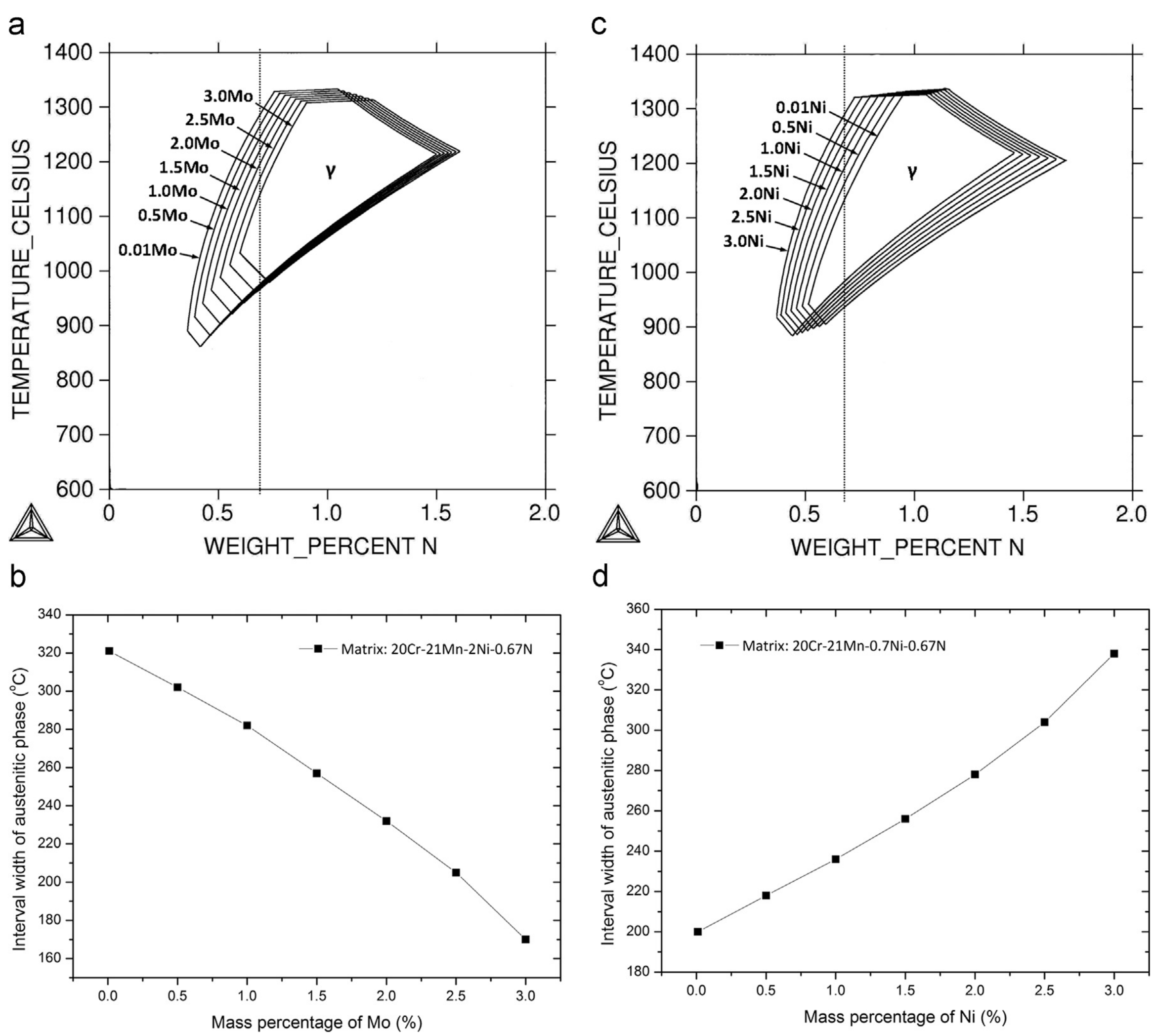

Fig. 2. Thermal dynamic calculation result:the effect of Mo on γ phase region (a) and temperature interval width (b); the effect of Ni on γ phase region (c) and temperature interval width (d).